AIP Applied Physics Letters

Anisotropic optical transmission of femtosecond laser induced periodic surface nanostructures on indium-tin-oxide films

Chih Wang, Hsuan-I Wang, Chih-Wei Luo, and Jihperng Leu

Citation: Applied Physics Letters **101**, 101911 (2012); doi: 10.1063/1.4751983
View online: http://dx.doi.org/10.1063/1.4751983
View Table of Contents: http://scitation.aip.org/content/aip/journal/apl/101/10?ver=pdfcov
Published by the AIP Publishing

Anisotropic optical transmission of femtosecond laser induced periodic surface nanostructures on indium-tin-oxide films

Chih Wang,[1] Hsuan-I Wang,[2] Chih-Wei Luo,[2,a)] and Jihperng Leu[1,b)]
[1]*Department of Materials Science and Engineering, National Chiao Tung University, Hsinchu 300, Taiwan*
[2]*Department of Electrophysics, National Chiao Tung University, Hsinchu 300, Taiwan*

(Received 9 July 2012; accepted 27 August 2012; published online 7 September 2012)

Two types of periodic nanostructures, self-organized nanodots and nanolines, were fabricated on the surfaces of indium-tin-oxide (ITO) films using femtosecond laser pulse irradiation. Multiple periodicities (approximately 800 nm and 400 nm) were clearly observed on the ITO films with nanodot and nanoline structures and were identified using two-dimensional Fourier transformation patterns. Both nanostructures show the anisotropic transmission characteristics in the visible range, which are strongly correlated with the geometry and the metallic content of the laser-induced nanostructures. © *2012 American Institute of Physics*. [http://dx.doi.org/10.1063/1.4751983]

Over the last decade, the appearance of materials has usually been engineered by modifying their surface morphology, such as thin-film coatings[1,2] and decorative etching,[3] or by forming one-dimensional gratings.[4–6] Recently, with the introduction of femtosecond (fs) laser amplifier, microstructures on the surface of materials or inside materials can be fabricated by illuminating with a femtosecond pulse laser,[7–9] which extensively modifies the electromagnetic wave at certain wavelengths. For example, colorizing metals[7] and black metals[8] are fabricated through a laser-induced periodic structure (LIPSS) on the surface of materials using fs pulse irradiation. Earlier studies mostly focused on altering the reflection and/or the absorption spectra of opaque materials; however, few studies addressed the modification of optical properties in transparent materials using fs laser pulses.[10] Xu *et al.*[11] recently fabricated large-area LIPSSs on zinc-oxide (ZnO) material using fs laser pulses. Moreover, they produced two-dimensional periodic nanostructures on ZnO crystal through two-beam interference of fs pulses[12] and subsequently enhanced its optical absorption in the visible range.[10] However, these results can only be achieved using high laser fluences (0.1–0.4 J/cm^2) with a focused spot of 100 μm, because of the pulse broadening after an objective, which further limits the large-area applications. In addition, the optical characteristics of nanostructures induced by fs laser pulses remain unclear.

According to the results for ZnO,[10–12] other transparent conducting oxide materials may have similar phenomena and applications. Indium-tin-oxide (ITO) is a well-known wide bandgap semiconductor that has metal-like electrical properties and high optical transmission in the visible region. In particular, ITO coated glass has been widely used as a transparent conductor in thin film transistors[13] and organic light-emitting devices (OLEDs).[14] The superior local conductivity in self-organized nanodots on ITO films induced by fs laser pulses was recently reported.[15] This periodic surface nanostructure can be fabricated with a relatively large area (over 0.2 mm × 0.2 mm in the center of beam spot) using low-fluence (<0.02–0.2 mJ/cm^2) fs laser pulses without scanning and an objective to maintain the pulse width in several tens of fs at the position of samples. This study also reports the anisotropic optical transmission of ITO films with periodic nanodot and nanoline structures, which are generated using a fs laser surface structuring technique by controlling the laser fluences and the number of shots. In addition, we discussed the relationship between the anisotropic optical transmission and the laser induced surface features (such as the shape, composition, size, and size distribution of the surface nanostructures).

ITO thin films with a thickness of 70 nm and an optimal resistivity of approximately 7×10^{-4} Ω-cm [$O_2/(O_2 + Ar)$ flow ratio of approximately 0.032] were deposited on glass substrates (1 cm × 1 cm) using magnetron sputtering deposition with 1000 W power. The ITO target (58 cm × 15 cm) consisted of In_2O_3 with 10 wt. % SnO_2. After the deposition of ITO films at room temperature, these samples were irradiated with normal incidence using a regenerative amplified Ti:sapphire laser (Legend USP, Coherent) with 800-nm wavelength, approximately 50-fs pulse duration, approximately 0.5-mJ pulse energy, and 5-kHz repetition rate. The diameter of the laser beam was adjusted to approximately 14 mm to ensure full exposure for a sample size of 1 cm × 1 cm. After irradiation, the sample was dipped in ethanol and cleaned for 10 min using an ultrasonic cleaner. The morphologies of the ITO films were examined using a scanning electron microscope (SEM, HITACHI-S2500 JSM-6500 F). The size distribution of the nanodots and nanolines in the SEM images in Figs. 1(a) and 1(b) was further analyzed and compiled using IMAGE J software, which is a public domain Java image processing program (available from US National Institutes of Health). The optical transmission measurements were performed using an UV-visible-near-IR spectrophotometer (JASCO V670). All optical spectra in this study were measured through an iris with a 0.1-mm diameter hole located at a position close to the central region of the laser-induced nanostructures (or laser spot). Polarizers were used during the optical measurements of the anisotropic optical transmission spectra. The local compositions of as-deposited and fs laser-treated ITO films with nanoline structures were examined using Auger electron spectroscopy (AES, ULVAC-PHI 700). Because of the spot size yielded

a)Electronic mail: cwluo@mail.nctu.edu.tw.
b)Electronic mail: jimleu@mail.nctu.edu.tw.

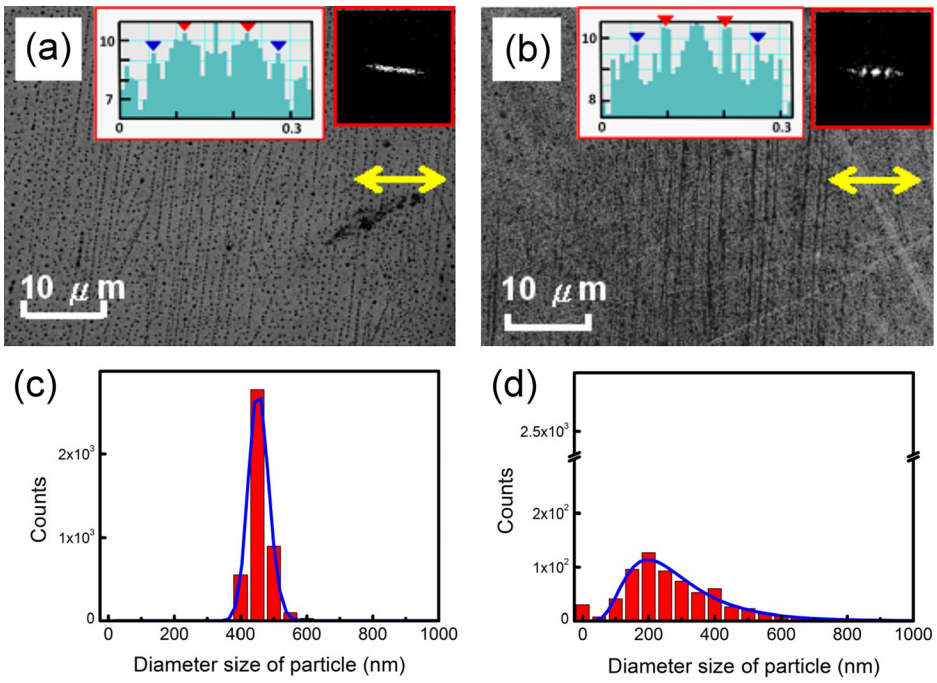

FIG. 1. SEM images (obtained from the central area in the 1×1-cm ITO films) of the periodic (a) nanodot and (b) nanoline structures induced by fs laser pulses with fluences (pulse numbers) of $F = 0.1$ mJ/cm^2 ($N = 3 \times 10^6$) and 0.2 mJ/cm^2 ($N = 2 \times 10^7$), respectively. The red-square insets show the 2D Fourier-transformed patterns and their cross-sectional profiles at locations corresponding to (a) and (b). The arrows indicate the direction of the laser polarization. The size distribution of particles for (c) nanodot structure in (a) and (d) nanoline structure in (b). The solid lines show the fitting curves using a log-normal function.

by an integral electron gun with an operating voltage of 5 KeV, the data collected by a cylindrical mirror analyzer had a spatial resolution of approximately 30 nm.

Figs. 1(a) and 1(b) show typical SEM images of ITO films with self-organized periodic nanodot and nanoline structures produced by linearly polarized fs laser pluses. Both types of periodic nanostructures can be easily and reliably obtained by precisely controlling the fluences (F) and number (N) of fs pulses. For the case of $F = 0.1$ mJ/cm^2 and $N = 3 \times 10^6$, the self-organized periodic nanodot structure with a size of a few hundred nanometers was observed on the surface of the ITO films. The periodicity of these nanodot structures was further estimated by the two-dimensional Fourier transformation (2D-FT), as shown in the inset of Fig. 1(a). From the positions of the satellite peaks in the 2D-FT pattern, two types of periodicities were observed in the laser-induced nanodot structures, that is, 816 ± 42 and 410 ± 30 nm. These periodicities can be attributed to the interference between the incident and scattered fs laser pluses.[15] An increase in the fluence to $F = 0.2$ mJ/cm^2 and the number of shots to $N = 2 \times 10^7$ caused the surface microstructure of ITO films to assume a periodic, line-like nanostructure (or nanoline structure), as shown in Fig. 1(b). In its corresponding 2D-FT pattern (the inset of Fig. 1(b)), a considerable reduction in the width of satellite peaks was observed, corresponding to a typical feature of a periodic line-like structure. The multiple spacings of 830 ± 12 and 455 ± 16 nm in the periodic nanoline structure were further estimated from the positions of the satellite peaks in a 2D-FT pattern. In addition, the direction of the 2D-FT pattern indicates that the periodic nanodot and nanoline structures were only generated in one direction, perpendicular to the direction of fs laser polarization (the arrows in Fig. 1). In short, the periodic nanodot or nanoline surface structures with periodicities of approximately 800 and 400 nm can be simply fabricated by precisely controlling the laser fluences and the number of shots.

The distribution of particle size for the nanodot and the nanoline structures on the surface of ITO films can be further counted by using IMAGE J software, as shown in Figs. 1(c) and 1(d). For the case of the nanodot structure in Fig. 1(c), the density of the dots was considerably high (approximately 1.94 count/μm^2), and the major size distribution of the dots was in the range of 300–500 nm with a high count of approximately 2500. However, a substantial reduction in the density of the dots (approximately 0.37 count/μm^2) was observed in the nanoline structure (Fig. 1(d)). A few unreasonable particle sizes of $1-2\,\mu$m (the enlarged scale plot is not shown here) were observed because of an erroneous judgment by the software, which estimates the size of a line pattern by a circle. Thus, the primary size distribution of the real dots was reduced to the range of 100–200 nm with a low count of 120.

According to Heilmann *et al.*,[16,17] the size, shape, and structural arrangement of the nanoparticles in materials result in changes of the optical properties, such as anisotropic reflectance and transmittance. Fig. 2(a) shows the nonpolarized optical properties of an as-deposited ITO film and the linear-polarized optical transmission properties of fs laser-treated ITO films with two types of surface nanostructures corresponding to the SEM images in Figs. 1(a) and 1(b), respectively. For an as-deposited ITO film, the nonpolarized transmission spectrum (a solid line in Fig. 2(a)) represents the standard optical properties in the visible range. For the fs laser-treated ITO films, the transmission spectra were measured using polarized light with a direction of polarization (P) parallel or perpendicular to the direction of the long-axis of the nanolines (L) on the ITO films (the inset of Fig. 2(a)). The transmission spectra were dependent on the orientation, that is, the transmission of L//P ($T_{L//P}$) for visible light was lower than that of L⊥P ($T_{L\perp P}$) in the fs laser irradiated ITO films with a nanodot structure. The difference between the transmittances, L//P ($T_{L//P}$) and L⊥P ($T_{L\perp P}$), for visible light was considerably larger in the fs laser irradiated

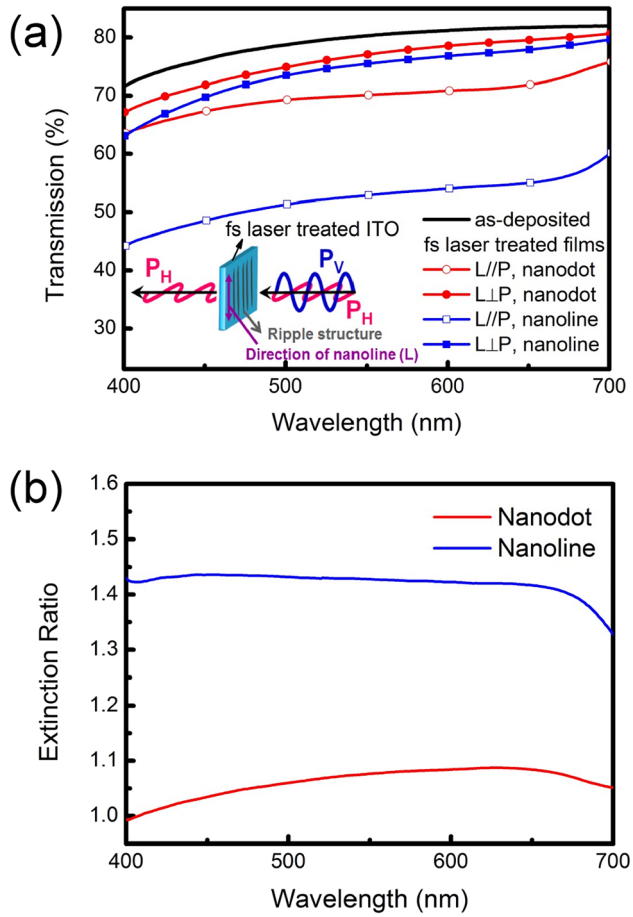

FIG. 2. (a) The optical transmission spectra of as-deposited ITO and fs laser-treated films with two types of nanostructures (nanodot and nanoline); the corresponding SEM images are shown in Figs. 1(a) and 1(b). The inset shows a schematic illustration of the two forms of polarized light (P_V and P_H) passing through a fs laser-treated ITO film. L: the direction of nanolines. (b) The extinction ratio ($T_{L\perp P}/T_{L//P}$) for the fs laser treated films with nanodot and nanoline structures. $T_{L\perp P}$ ($T_{L//P}$) is the transmittance in the configuration, L⊥P (L//P).

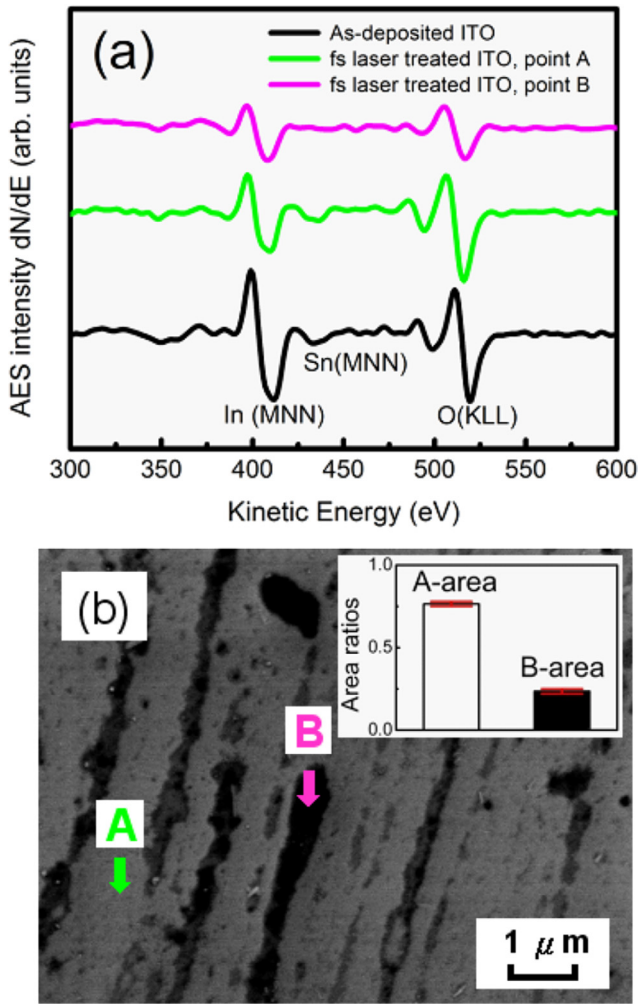

FIG. 3. (a) The first derivative (dN/dE) of AES peaks, In(MNN), Sn(MNN), and O(KLL), measured for an as-deposited ITO film and a fs laser treated ITO film with a nanoline structure. The point A (outside a nanoline) and point B (inside a nanoline) correspond to the arrows marked in (b), the SEM image of a fs laser treated ITO film. The inset shows the ratio of the areas of the as-deposited (A-area) region and the nanoline (B-area) region.

ITO films with a nanoline structure. The extinction ratio ($T_{L\perp P}/T_{L//P}$) in the ITO films with a nanoline structure was enhanced by 42% at a wavelength of 400 nm, as shown in Fig. 2(b). This dichroic or anisotropic transmission property of the fs laser-treated ITO films can be attributed to the laser-induced periodic nanostructures on their surfaces. The inset of Fig. 2(a) shows a schematic illustration for the dichroic optical property of fs laser-treated ITO films with a nanoline structure. The fs laser-treated ITO film blocks the vertically polarized light (P_V), which is parallel to the long axis of the nanoline structure (L). The horizontally polarized light (P_H) can pass through the nanoline structure, which is perpendicular to the long axis of the nanoline structure (L). These results indicate that anisotropic optical transmission can be simply constructed and manipulated in ITO films using fs laser irradiation. This property may have potential in applications such as optical devices for polarization control in the visible range.[18] The anisotropic reflection property of fs laser-treated ITO films was not evident (not shown here) because of a relatively low reflectance compared to the transmittance for an optimal ITO film.

To determine the mechanism responsible for the anisotropic optical properties of fs laser-treated ITO films, the composition of nanostructures in ITO films was examined using AES. Fig. 3 shows the first derivative (dN/dE) of the AES peaks, including In(MNN), Sn(MNN), and O(KLL) of an as-deposited and a fs laser-treated ITO film with a nanoline structure. For the as-deposited ITO film [bottom-black line in Fig. 3(a)], three dN/dE signals can be assigned to In(MNN) at a kinetic energy of 410 eV,[19] Sn(MNN) at a kinetic energy of 433 eV,[19,20] and O(KLL) at a kinetic energy of 519 eV,[19,21] respectively. For the fs laser-treated ITO film, the dN/dE signals of In(MNN), Sn(MNN), and O(KLL) at point A in Fig. 3(b) were slightly reduced compared with those for an as-deposited ITO film. However, the dN/dE signals (top-pink line in Fig. 3(a)) reduced considerably at point B in Fig. 3(b), which is located within the lines induced by the fs laser pulses. The reduction in signals was most substantial for the dN/dE signals of Sn(MNN) and O(KLL). This implies that the composition of ITO films is modified by fs laser annealing, particularly at the locations of the lines. According to our previous findings,[15] the composition of the fs laser-induced nanoline structure on the surface of an ITO film deviates from the stoichiometry of the as-deposited ITO films. A further examination of the peak intensities of

the as-deposited and fs laser treated ITO films showed that the *dN*/*dE* peak intensity ratio for O(KLL) to In(MNN) changed from 1.7 to 1.1 (approximately 36% reduction) after fs laser irradiation. Moreover, the metal content in the nanolines was higher than that in the nanodots (approximately 23% reduction of oxygen content), as reported in our previous study.[15] Consequently, the ITO films with a nanoline structure functioned similarly to a wire grid plate with a regular grid of metallic wires. For the case of L//P in Fig. 2(a), the incoming electromagnetic (EM) wave was reflected or absorbed by the metallic and periodic nanoline structure on the ITO films because of the movement of electron along the metallic nanolines and Joule heating loss, which leads to blocking of the EM wave. However, an EM wave with L⊥P cannot induce electron movement along the metallic nanolines in the same manner. Therefore, the loss caused by Joule heating and reflection is limited and the EM wave is transmitted through the periodic nanoline structure on ITO films.

Finally, the inset in Fig. 3(b) shows a bar chart for the ratios of the areas of the nanolines (B-area) and the as-deposited region (A-area), as estimated from Fig. 3(a). The nanolines occupied 23.5% ± 1.1% of the total area, as calculated using the IMAGE J software. However, the nanoline structure on the surface of the ITO films cannot block all of the light. Even for a metal-like ITO film in which the $O_2/(O_2 + Ar)$ flow ratio is 0 (its optical transmittance spectrum is not shown here), the transmittance at a wavelength of 500 nm was approximately 42%. For comparison, the transmission of the as-deposited ITO film was 78% at a wavelength of 500 nm. Therefore, the transmission of ITO films with a nanoline structure, in which 23.5% is metal-like lines area and 76.5% is as-deposited area, was estimated at approximately 69.5%. However, a low transmittance of approximately 52% for L//P and a high transmittance of approximately 74% for L⊥P were observed in the transmission spectra, as shown in Fig. 2(a). This strongly implies that the increase in metallic content cannot explain the optical transmission property of ITO films with nanostructures. Thus, the geometric effect of nanostructures may dominate the anisotropic transmission property of fs laser irradiated ITO films.

Two types of nanostructures, nanodots and nanolines, with multiple periodicities of approximately 800 and 400 nm can be simply and reliably fabricated on ITO films using fs laser pulse irradiation with various fluences and number of shots. Both nanostructures show anisotropic characteristics in their optical transmission spectra in the visible range, especially the nanoline structures. Moreover, the extinction ratio of ITO films with nanostructures can be enhanced with nanoline structures by increasing the laser fluences and the number of shots. In summary, ITO films with unique optical transmission properties can be fabricated using this simple method and has considerable potential in optoelectronics applications for polarizing optical elements and smart window technology in the visible spectroscopy.

The authors thank the National Science Council of Taiwan for the financial support under Grant Nos. NSC 101-3113-E-007-001- and NSC 101-2112-M-009-016-MY2. The assistance of Paragon Technology Corp. for the magnetron sputter is also acknowledged.

[1]J. W. Nah, B. J. Kim, D. K. Lee, and J. J. Lee, J. Vac. Sci. Technol. A **17**, 463 (1999).
[2]E. E. Salagean, D. B. Lewis, J. S. Brooks, W. D. Münz, I. Petrov, and J. E. Greene, Surf. Coat. Technol. **82**, 57 (1996).
[3]C. Hemmingsson, P. P. Paskov, G. Pozina, M. Heuken, B. Schineller, and B. Monemar, Superlattices Microstruct. **40**, 205 (2006).
[4]P. Sheng, A. N. Bloch, and R. S. Stepleman, Appl. Phys. Lett. **43**, 579 (1983).
[5]P. J. Hesketh, J. N. Zemel, and B. Gebhart, Phys. Rev. B **37**, 10795 (1988).
[6]S. Hava, J. Ivri, and M. Auslender, J. Appl. Phys. **85**, 7893 (1999).
[7]Y. Vorobyev and C. Guo, Appl. Phys. Lett. **92**, 041914 (2008).
[8]Y. Vorobyev and C. Guo, Opt. Photonics News **18**, 43 (2007).
[9]C. W. Luo, C. C. Lee, C. H. Li, H. C. Shih, Y. J. Chen, C. C. Hsieh, C. H. Su, W. Y. Tzeng, K. H. Wu, J. Y. Juang, T. M. Uen, S. P. Chen, J.-Y. Lin, and T. Kobayashi, Opt. Express **16**, 20610 (2008).
[10]X. Jia, T. Jia, Y. Zhang, P. Xiong, D. Feng, Z. Sun, and Z. Xu, Opt. Express **18**, 14401 (2010).
[11]M. Huang, F. Zhao, Y. Cheng, N. Xu, and Z. Xu, Opt. Express **16**, 19354 (2008).
[12]T. Jia, M. Baba, M. Suzuki, R. A. Ganeev, H. Kuroda, J. Qiu, X. Wang, R. Li, and Z. Xu, Opt. Express **16**, 1874 (2008).
[13]C. E. Kim and I. Yun, Appl. Phys. Lett. **100**, 013501 (2012).
[14]Y. Zhao, L. Duan, D. Zhang, L. Hou, J. Qiao, L. Wang, and Y. Qiu, Appl. Phys. Lett. **100**, 083304 (2012).
[15]C. Wang, H. I. Wang, C. W. Luo, T. Kobayashi, and J. Leu, Opt. Express **19**, 24286 (2011).
[16]M. Kaempfe, H. Graener, A. Kiesow, and A. Heilmann, Appl. Phys. Lett. **79**, 1876 (2001).
[17]K. Loeschner, G. Seifert, and A. Heilmann, J. Appl. Phys. **108**, 073114 (2010).
[18]J. Elliott, I. I. Smolyaninov, N. I. Zheludev, and A. V. Zayats, Opt. Lett. **29**, 1414 (2004).
[19]J. A. Chaney and P. E. Pehrsson, Appl. Surf. Sci. **180**, 214 (2001).
[20]D. Briggs and M. P. Seah, *Practical Surface Analysis* (John Wiley and Sons, New York, 1993).
[21]F. Zhu, C. H. A. Huan, K. Zhang, and A. T. S. Wee, Thin Solid Films **359**, 244 (2000).